

Hybrid Quantum-Classical Machine Learning with String Diagrams

Alexander Koziell-Pipe

University of Oxford
Oxford, UK

`alexander.koziell-pipe@cs.ox.ac.uk`

Aleks Kissinger

University of Oxford
Oxford, UK

`aleks.kissinger@cs.ox.ac.uk`

Central to near-term quantum machine learning is the use of hybrid quantum-classical algorithms. This paper develops a formal framework for describing these algorithms in terms of string diagrams: a key step towards integrating these hybrid algorithms into existing work using string diagrams for machine learning and differentiable programming. A notable feature of our string diagrams is the use of functor boxes, which correspond to a quantum-classical interfaces. The functor used is a lax monoidal functor embedding the quantum systems into classical, and the lax monoidality imposes restrictions on the string diagrams when extracting classical data from quantum systems via measurement. In this way, our framework provides initial steps toward a denotational semantics for hybrid quantum machine learning algorithms that captures important features of quantum-classical interactions.

1 Introduction

At time of writing, we are still in the Noisy Intermediate Scale (NISQ) era of quantum computing[29], where techniques to correct errors are still under development and the size of quantum circuits are limited. Quantum algorithms requiring deep circuits and larger numbers of qubits, notably Shor’s[34, 33] and Grover’s[19] algorithms, are still beyond our reach for practical use.

Hybrid quantum-classical algorithms, where quantum computations interoperate with classical, offer a pragmatic solution to these limitations. These hybrid algorithms extract as much performance as possible out of limited quantum resources by delegating a large part of their computation to classical computers, then using quantum processors for small subroutines for which they are particularly well-suited.

The archetypal example of hybrid algorithms in the context of quantum machine learning is the Variational Quantum Eigensolver[27] and more generally, Variational Quantum Algorithms[7]. In these algorithms a parameterized quantum circuit is used to compute a cost function, which is provided to a classical optimizer that computes updated parameters to minimize the cost. Computing updated parameters may involve further quantum processing in order to evaluate gradients of the cost function with respect to the parameters[25, 30]. This process is repeated iteratively until a desired performance or termination condition is met. These algorithms are inherently hybrid in the sense of [6], as they require non-trivial amounts of both quantum and classical computational resources to run. Furthermore, they involve the repeated transfer of information between quantum and classical systems.

In this work, we provide a diagrammatic formalism of hybrid algorithms using category theory. Originally developed to study algebraic topology[13], category theory has since found applications across a range of scientific disciplines, including quantum computing[3, 4, 10] and machine learning[15, 12, 18]¹.

¹For references spanning a range of machine learning topics, see [17].

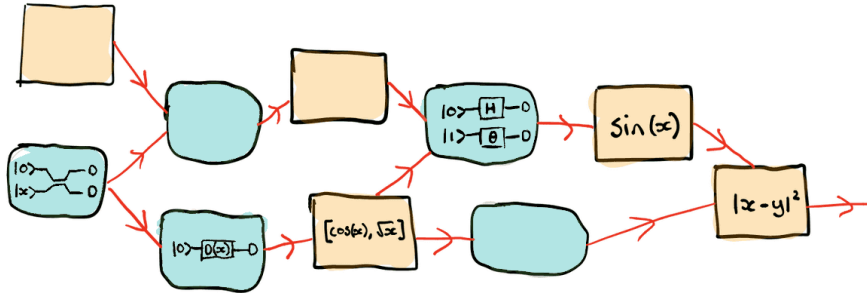


Figure 1: From [1]. An informal schematic of the flow of information between classical and quantum nodes. Our work aims to formalize this in terms of category theory, allowing it to be depicted as a string diagram.

Category theory provides a unifying language for different branches of mathematics. Furthermore, it offers an abstract framework for understanding and formalizing different mathematical structures and the relationships between them. In the context of this paper, category theory bridges the gap between machine learning and quantum computing. The mathematics of machine learning is characterised by smooth, differentiable functions and the ability to freely copy and delete information without restriction. This sits in stark contrast with quantum computation, where calculating gradients of arbitrary quantum circuits is highly non-trivial, and copying and deleting information is physically prohibited by the no-cloning and no-deleting theorems of quantum information.

This separation between the mathematics of machine learning and quantum computing is reflected by the distinct properties of the categories in which each are described. While categorical quantum mechanics is formulated in terms of dagger compact closed categories, the categorical machine learning typically uses Cartesian categories in which there is a suitable notion of a reverse derivative. Our work is a step towards combining these two theories of systems and processes into a single framework, with the intention of facilitating seamless interoperability in practical implementations of hybrid quantum-classical algorithms.

Our contributions are as follows. First, following[12], we establish the Cartesian category Smooth as the category with which to describe the classical part of our algorithms. Next, we choose the compact closed category $\text{CPM}(\text{FHilb}_{\mathbb{C}})$ of completely positive maps[32] for the quantum part. We then show that there exists a lax monoidal functor $F : \text{CPM}(\text{FHilb}_{\mathbb{C}}) \rightarrow \text{Smooth}$, which we define as the composition of two functors $G : \text{CPM}(\text{FHilb}_{\mathbb{C}}) \rightarrow \text{Mat}_{\mathbb{R}}$ and $H : \text{Mat}_{\mathbb{R}} \rightarrow \text{Smooth}$. We give a concrete description of this functor by fixing a basis in terms of Pauli operators for each object of $\text{CPM}(\text{FHilb}_{\mathbb{C}})$. The lax monoidal functor bridges our quantum and classical systems, and allows the description of hybrid classical-quantum algorithms using string diagrams[31, 28] in which functorial boxes[8, 24] represent classical-quantum interfaces. The lax condition on our functor allows multiple wires to enter the box, representing the encoding of classical data into the quantum circuit, but only one wire to exit, representing a measurement probability. Furthermore, we are able to represent the quantum system as a ZX-diagram[9, 36, 2], making the quantum part of our algorithm amenable to quantum circuit optimization methods. Finally, we show a concrete application of our framework to the quantum machine learning algorithm of [14], in which parameterized quantum circuits are trained on MNIST classification[22]. Our framework gives us a denotational semantics of this quantum machine learning algorithm that could form the basis of a programming language for quantum machine learning, or hybrid quantum-classical

algorithms more generally.

Our work is intended as a step toward the extension of categorical gradient based learning framework to allow ‘quantum nodes’, and future work will aim to formalise parameterization and backpropagation in these hybrid algorithms through the use of the parametric lens construction of [12] and diagrams for ‘gradient recipes’ [25, 30], an established method for computing the gradient of a parameterized quantum circuit for use in quantum machine learning.

2 Theory

In this section, we define categories $\text{CPM}(\text{Qubit})$ and Smooth for quantum and classical systems. We then show that there is a lax monoidal functor $F: \text{CPM}(\text{Qubit}) \rightarrow \text{Smooth}$. We define as the composition of two functors $G: \text{CPM}(\text{Qubit}) \rightarrow \text{Mat}_{\mathbb{R}}$ and $H: \text{Mat}_{\mathbb{R}} \rightarrow \text{Smooth}$, using the category $\text{Mat}_{\mathbb{R}}$ of real matrices as an intermediate step in the passage from quantum to classical systems.

For a brief review of categories and functors, see section A.1 of the appendix. For a further introduction to category theory see, for example, [23, 16].

2.1 $\text{FHilb}_{\mathbb{C}}$ and ZX-diagrams

Pure state quantum mechanics can be described mathematically in terms of complex Hilbert spaces. Furthermore, in quantum computing we are usually interested in finite-dimensional systems. As a consequence, much of the work applying category theory to quantum mechanics involves the use of the category $\text{FHilb}_{\mathbb{C}}$:

Definition 1 ($\text{FHilb}_{\mathbb{C}}$). The symmetric monoidal category $\text{FHilb}_{\mathbb{C}}$ is defined by:

Objects finite-dimensional complex Hilbert spaces.

Morphisms $H \rightarrow K$ linear maps from H to K .

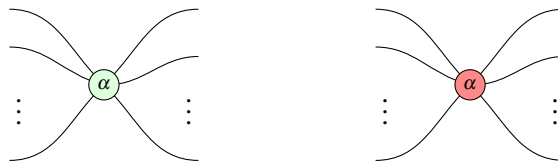
Monoidal product the tensor product of Hilbert spaces.

Monoidal unit the 0-dimensional Hilbert space.

When working with quantum computation, in particular qubits, we can simplify the objects we have to work with by moving to the subcategory of $\text{FHilb}_{\mathbb{C}}$ consisting of products of 2-dimensional complex spaces $(\mathbb{C}^2)^{\otimes n}$. We call this category Qubit and define it as a PROP:

Definition 2 (Qubit). The category Qubit is the PROP whose morphisms $n \rightarrow m$ are given by $2^m \times 2^n$ complex matrices, $\text{Qubit}(n, m) := \mathbb{M}_{\mathbb{C}}^{2^m \times 2^n}$. The monoidal product on morphisms is given by the Kronecker product of matrices.

We can think of the objects $n \in \text{Qubit}$ as corresponding to Hilbert spaces $(\mathbb{C}^2)^{\otimes n}$ containing the complex amplitudes for an n -qubit system. When working in Qubit , we can use ZX-diagrams [9, 36, 2] to describe our morphisms. ZX-diagrams are generated by green (light) Z spiders and red (dark) X spiders, corresponding to the quantum states $|00\dots 0\rangle\langle 00\dots 0| + e^{i\alpha}|11\dots 1\rangle\langle 11\dots 1|$ and $|+\dots+\rangle\langle +\dots+| + e^{i\alpha}|-\dots-\rangle\langle -\dots-|$, respectively:



Any morphism in Qubit can be expressed as (possibly multiple) ZX-diagram(s). Furthermore, the diagrams can be equipped with a set of rewrite rules allowing one diagram to be transformed into another. There are known sets of rewrite rules that are sound and complete, meaning that two diagrams can be transformed into one another if and only if they correspond to the same quantum process. ZX-diagrams together with a canonical set of rewrite rules are referred to as the ZX-calculus, and has useful applications to quantum circuit simplification and quantum error correction. For a more in-depth introduction, see [36].

2.2 CPM(FHilb $_{\mathbb{C}}$) and Doubled ZX

When bridging from quantum to classical systems, we will choose to work with the density operator formalism of quantum mechanics. This allows us to work with mixed-state quantum mechanics, as well as express our diagrams using a basis of Pauli operators with real coefficients. This requires deriving a different category from FHilb $_{\mathbb{C}}$, using the CPM-construction of [32]. When applied to FHilb $_{\mathbb{C}}$, this gives us the following category, where we denote the space of linear operators on a Hilbert space H by $\mathcal{L}(H)$:

Definition 3. The category CPM(FHilb $_{\mathbb{C}}$) is defined by

Objects complex Hilbert spaces.

Morphisms $H \rightarrow K$ completely positive linear superoperators $\mathcal{L}(H) \rightarrow \mathcal{L}(K)$.

Like FHilb $_{\mathbb{C}}$, CPM(FHilb $_{\mathbb{C}}$) is symmetric monoidal, with monoidal product given by the tensor product. If we once again restrict to 2-dimensional complex Hilbert spaces, we can similarly define CPM(Qubit):

Definition 4. The category CPM(Qubit) is the PROP whose morphisms $n \rightarrow m$ are the completely positive linear superoperators $\mathcal{L}((\mathbb{C}^2)^{\otimes n}) \rightarrow \mathcal{L}((\mathbb{C}^2)^{\otimes m})$.

Contrasting with Qubit, objects n of CPM(Qubit) can be thought of as corresponding to spaces $(\mathbb{C}^2)^{\otimes n} \otimes (\mathbb{C}^2)^{\otimes n} := \mathbb{C}^{2^n \times 2^n}$. States (morphisms $0 \rightarrow n$ for some $n \in \text{Qubit}$) correspond to density matrices, while processes $n \rightarrow m$ correspond to quantum channels.

We can extend the ZX-calculus to CPM(Qubit) through a process known as ‘doubling’ [10, Chapter 8]. In this doubled notation, thick (‘doubled’) wires correspond to quantum systems and thin single wires correspond to classical ones. Z and X spiders in this doubled notation are defined in terms of their undoubled counterparts as follows:

$$\begin{array}{c} \text{Thick Z Spider} \\ \vdots \end{array} := \begin{array}{c} \text{Thin X Spiders} \\ \vdots \end{array} \quad \begin{array}{c} \text{Thick X Spider} \\ \vdots \end{array} := \begin{array}{c} \text{Thin Z Spiders} \\ \vdots \end{array} \quad (1)$$

In addition, we gain a ‘decoherence’ operation, defined by:

$$\text{Thick wire splitting to thin wires} := \text{Thick wire loop} \quad (2)$$

In terms of density operators and superoperators, we can regard this decoherence operator as taking the trace, or partial trace if applied to a single output of a multiple-output diagram. In the context of

quantum circuits, this operation can be thought of as discarding the measurement result on a qubit, and is often referred to as the ‘discard’ operation.

These doubled ZX diagrams live in their own PROP, which we denote ZX_{\ddagger} . There is then an interpretation functor $\llbracket - \rrbracket : ZX_{\ddagger} \rightarrow \text{CPM}(\text{Qubit})$ that maps a doubled ZX diagram to the completely positive map it corresponds to.

2.3 Smooth

We describe the classical part of our machine learning algorithms using the category Smooth of smooth maps between Euclidean spaces. We choose to define Smooth as a PROP, with objects n corresponding to Euclidean spaces \mathbb{R}^n :

Definition 5. The category Smooth is the PROP with morphisms $n \rightarrow m$ tuples of smooth maps $f := (f_1, \dots, f_m) : \mathbb{R}^n \rightarrow \mathbb{R}^m$. The monoidal product of two morphisms $f : n \rightarrow m$ and $g : n' \rightarrow m'$ is obtained by concatenating the output of f (an m -tuple) on the first n elements of $\mathbb{R}^{n+n'}$ with the output of g (an m' -tuple) on the last n' elements.

2.4 Bridging from Quantum to Classical

In order to combine quantum and classical systems in the same string diagrams, we must define a functor $F : \text{CPM}(\text{Qubit}) \rightarrow \text{Smooth}$. To this end, we first introduce the PROP $\text{Mat}_{\mathbb{R}}$:

Definition 6. The category $\text{Mat}_{\mathbb{R}}$ is the PROP whose morphisms $n \rightarrow m$ are the real $m \times n$ matrices $\mathbb{M}_{\mathbb{R}}^{m \times n}$. The monoidal product on morphisms is given by the Kronecker product of matrices.

Next, we define a functor $G : \text{CPM}(\text{Qubit}) \rightarrow \text{Mat}_{\mathbb{R}}$, which allows us to express quantum computations using real matrices. First, note that a completely positive superoperator $\mathcal{L}(\mathbb{C}^{2^n}) \rightarrow \mathcal{L}(\mathbb{C}^{2^m})$ is uniquely determined by a real matrix with respect to the n and m -tensor products of Pauli matrices.

Definition 7. The functor $G : \text{CPM}(\text{Qubit}) \rightarrow \text{Mat}_{\mathbb{R}}$ is defined by the following mappings:

Objects $n \mapsto 4^n$.

Morphisms A completely positive map $\mathcal{L}(\mathbb{C}^{2^n}) \rightarrow \mathcal{L}(\mathbb{C}^{2^m})$ is mapped to the $m \times n$ real matrix with respect to the m - and n -tensor Pauli bases.

As an example, consider the quantum state $|0\rangle + e^{i\alpha}|1\rangle$. Ignoring global scalar factors and working in the computational basis, the density operator for this state is:

$$\begin{pmatrix} 1 & e^{-i\alpha} \\ e^{i\alpha} & 1 \end{pmatrix} = I + \cos(\alpha)\sigma_x + \sin(\alpha)\sigma_y$$

Where I is the identity matrix and σ_i are the Pauli matrices. This would correspond to the following doubled ZX diagram:



Interpreting this diagram in $\text{CPM}(\text{Qubit})$ and applying G , this would become:

$$G \llbracket \text{⊙} \text{---} \rrbracket = \begin{pmatrix} 1 \\ \cos(\alpha) \\ \sin(\alpha) \\ 0 \end{pmatrix} \quad (3)$$

More generally, we can derive real matrices for completely positive maps as follows. For each $n \in \mathbb{N}$, fix an ordering on the n -qubit Pauli operators ² and label them according to this order as σ_i^n for $i \in \{0, 1, \dots, 4^n - 1\}$. Then entries of the matrix M of a completely positive superoperator $\Phi : n \rightarrow m$ are obtained via:

$$M_{ij} = \text{tr} \left((\sigma_i^m)^\dagger \cdot \Phi(\sigma_j^n) \right) \quad (4)$$

Given a Kraus decomposition of the operator Φ , this can be calculated numerically. For example, we can use (4) to derive real matrices for the state $|+\rangle + e^{i\alpha}|-\rangle$:

$$G \left[\begin{array}{c} \text{---} \textcircled{\alpha} \text{---} \end{array} \right] = \begin{pmatrix} 1 & & & \\ & 0 & & \\ & -\sin(\alpha) & & \\ & \cos(\alpha) & & \end{pmatrix} \quad (5)$$

as well as R_Z, R_X ,

$$G \left[\begin{array}{c} \text{---} \textcircled{\alpha} \text{---} \end{array} \right] = \begin{pmatrix} 1 & 0 & 0 & 0 \\ 0 & \cos(\alpha) & -\sin(\alpha) & 0 \\ 0 & \sin(\alpha) & \cos(\alpha) & 0 \\ 0 & 0 & 0 & 1 \end{pmatrix} \quad (6)$$

$$G \left[\begin{array}{c} \text{---} \textcircled{\alpha} \text{---} \end{array} \right] = \begin{pmatrix} 1 & 0 & 0 & 0 \\ 0 & 1 & 0 & 0 \\ 0 & 0 & \cos(\alpha) & -\sin(\alpha) \\ 0 & 0 & \sin(\alpha) & \cos(\alpha) \end{pmatrix} \quad (7)$$

Hadamard,

$$G \left[\begin{array}{c} \text{---} \textcircled{\square} \text{---} \end{array} \right] = \begin{pmatrix} 1 & 0 & 0 & 0 \\ 0 & 0 & 0 & 1 \\ 0 & 0 & -1 & 0 \\ 0 & 1 & 0 & 0 \end{pmatrix} \quad (8)$$

and CNOT gates (where I and 0 are the 2×2 identity and zero matrices, respectively):

$$G \left[\begin{array}{c} \text{---} \textcircled{\text{green}} \text{---} \\ \text{---} \textcircled{\text{red}} \text{---} \end{array} \right] = \begin{pmatrix} I & 0 & 0 & 0 & 0 & 0 & 0 & 0 \\ 0 & 0 & 0 & 0 & 0 & 0 & 0 & I \\ 0 & 0 & 0 & 0 & 0 & 0 & 0 & 0 \\ 0 & 0 & 0 & 0 & 0 & -i\sigma_y & 0 & 0 \\ 0 & 0 & 0 & 0 & \sigma_x & 0 & 0 & 0 \\ 0 & 0 & 0 & i\sigma_y & 0 & 0 & 0 & 0 \\ 0 & 0 & 0 & 0 & 0 & 0 & I & 0 \\ 0 & I & 0 & 0 & 0 & 0 & 0 & 0 \end{pmatrix} \quad (9)$$

Remark 1. This construction could in principle be extended to qudits by using generalizations of Pauli matrices, see [20] and [5].

²For example, $(I \otimes I, I \otimes \sigma_X, I \otimes \sigma_Y, I \otimes \sigma_Z, \sigma_X \otimes I, \dots, \sigma_Z \otimes \sigma_Z)$ on the 2-qubit operators.

Now that we have a functor to go from our abstract quantum circuit representations in $\text{CPM}(\text{Qubit})$ to concrete matrices in $\text{Mat}_{\mathbb{R}}$, it remains to go from $\text{Mat}_{\mathbb{R}}$ to Smooth . This is done by the following functor:

Definition 8. The functor $H : \text{Mat}_{\mathbb{R}} \rightarrow \text{Smooth}$ is defined by the following:

Objects H is identity on objects $n \mapsto n$.

Morphisms $m \times n$ real matrices are mapped to the corresponding smooth map $\mathbb{R}^n \rightarrow \mathbb{R}^m$.

The composition of these two functors $F := G \circ H$ gives us a functor from quantum to classical, which we will use to draw a functor box in our string diagrams.

We now prove a theorem about our functor F , which will be of importance when constructing our quantum machine learning string diagrams.

We now prove that F is lax monoidal.

Theorem 1. *The functor F is lax monoidal.*

Proof. We begin by defining the coherence maps:

- The morphism $\varepsilon : 0 \rightarrow F(0) = 1$ is the map $\mathbb{R}^0 \rightarrow \mathbb{R}$ taking the single element $*$ to 1.
- We define the natural transformation $\mu_{n,m} : F(n) + F(m) \rightarrow F(n+m)$ by noting that in Smooth , the object $F(n) + F(m) = 4^n + 4^m$ corresponds to the Euclidean space $\mathbb{R}^{4^n+4^m}$. Elements of this space can be characterized by pairs of 4^n and 4^m -dimensional real vectors (\vec{v}, \vec{w}) . We map these to the space $\mathbb{R}^{4^{n+m}}$ corresponding to $F(n+m) = 4^{n+m}$ as follows:

$$(\vec{v}, \vec{w}) \mapsto \vec{v} \otimes \vec{w} \quad (10)$$

Where \otimes denotes the Kronecker product.

We now prove that these maps satisfy the coherence conditions. For clarity, we denote the monoidal product on morphisms as \otimes in $\text{CPM}(\text{Qubit})$ and as \times in Smooth , reflecting their operational behaviour.

- For associativity, we must show that the following diagram commutes:

$$\begin{array}{ccc} (F(n) + F(m)) + F(k) & \xrightarrow{\alpha^{\text{Smooth}}} & F(n) + (F(m) + F(k)) \\ \mu_{n,m} \times id_{F(k)} \downarrow & & \downarrow id_{F(n)} \times \mu_{m,k} \\ F(n+m) + F(k) & & F(n) + F(m+k) \\ \mu_{n+m,k} \downarrow & & \downarrow \mu_{n,m+k} \\ F((n+m) + k) & \xrightarrow{F(\alpha^{\text{CPM}(\text{Qubit})})} & F(n + (m+k)) \end{array} \quad (11)$$

Where α denotes the associators in Smooth and $\text{CPM}(\text{Qubit})$. Given that the associators in Smooth and $\text{CPM}(\text{Qubit})$ are trivial, we draw the simpler diagram:

$$\begin{array}{ccc} F(n) + F(m) + F(k) & \xrightarrow{id_{F(n)} \times \mu_{m,k}} & F(n) + F(m+k) \\ \mu_{n,m} \times id_{F(k)} \downarrow & & \downarrow \mu_{n,m+k} \\ F(n+m) + F(k) & \xrightarrow{\mu_{n+m,k}} & F(n+m+k) \end{array} \quad (12)$$

We prove this diagram commutes as follows. Assume any element $(\vec{u}, \vec{v}, \vec{w})$ from the top left of the square. The top corner of the square maps this element as follows:

$$(\vec{u}, \vec{v}, \vec{w}) \mapsto (\vec{u}, \vec{v} \otimes \vec{w}) \mapsto (\vec{u} \otimes (\vec{v} \otimes \vec{w})) \quad (13)$$

Conversely, the bottom corner of the square maps this element as follows:

$$(\vec{u}, \vec{v}, \vec{w}) \mapsto (\vec{u} \otimes \vec{v}, \vec{w}) \mapsto ((\vec{u} \otimes \vec{v}) \otimes \vec{w}) \quad (14)$$

These two mappings are equal by the associativity of the Kronecker product. Hence the square commutes.

- For unitality, we must show that the following diagrams commute:

$$\begin{array}{ccc} 0 + F(n) & \xrightarrow{\varepsilon \times id_{F(n)}} & F(0) + F(n) \\ \downarrow l^{\text{Smooth}} & & \downarrow \mu_{0,n} \\ F(n) & \xleftarrow{F(l^{\text{CPM(Qubit)})}} & F(0 + n) \end{array} \quad (15)$$

$$\begin{array}{ccc} F(n) + 0 & \xrightarrow{id_{F(n)} \times \varepsilon} & F(n) + F(0) \\ \downarrow r^{\text{Smooth}}_{F(n)} & & \downarrow \mu_{n,0} \\ F(n) & \xleftarrow{F(r_n^{\text{CPM(Qubit)})}} & F(n + 0) \end{array} \quad (16)$$

Where l and r denote left and right unitors, respectively. Take an element from the top left corner of the first square. Tracing the long route to the right, down, then left, we have:

$$(*, \vec{u}) \mapsto (1, \vec{u}) \mapsto 1 \otimes \vec{u} \mapsto \vec{u} \quad (17)$$

The route straight down maps the element as:

$$(*, \vec{u}) \mapsto \vec{u} \quad (18)$$

Thus the diagram commutes. The second diagram is similar. Along the right, down, left route:

$$(\vec{u}, *) \mapsto (\vec{u}, 1) \mapsto \vec{u} \otimes 1 \mapsto \vec{u} \quad (19)$$

Along the route straight down:

$$(\vec{u}, *) \mapsto \vec{u} \quad (20)$$

- It remains to show that μ is a natural transformation. For this we must prove that the following diagrams commute for all n, m, k and completely positive superoperators T, T' on the appropriate Hilbert spaces:

$$\begin{array}{ccc} F(n) + F(m) & \xrightarrow{\mu_{n,m}} & F(n + m) \\ \downarrow id_{F(n)} \times F(T) & & \downarrow F(id_n \otimes T) \\ F(n) + F(k) & \xrightarrow{\mu_{n,k}} & F(n + k) \end{array} \quad (21)$$

and

$$\begin{array}{ccc}
 F(n) + F(m) & \xrightarrow{\mu_{n,m}} & F(n+m) \\
 \downarrow F(T') \times id_{F(m)} & & \downarrow F(T' \otimes id_m) \\
 F(k) + F(m) & \xrightarrow{\mu_{n,k}} & F(k+m)
 \end{array} \tag{22}$$

We prove only that the first square commutes: the second is similar by the symmetry of the tensor and Cartesian products.

First notice that since G represents linear maps as matrices with respect to orthonormal bases, it preserves the tensor product: $G(T_1 \otimes T_2) = G(T_1) \otimes G(T_2)$ ³. Thus $F(id_n + T) = H \circ G(id_n \otimes T) = H(I_{4^n} \otimes M)$, where I_{4^n} is the $4^n \times 4^n$ identity matrix and M is the matrix for T with respect to the tensored Pauli bases.

Next note that since by definition of the tensor product, $(M_1 \otimes M_2)(\vec{u} \otimes \vec{v}) = M_1\vec{u} \otimes M_2\vec{v}$. Thus in order for the map $H(M_1 \otimes M_2)$ in Smooth to correspond to $M_1 \otimes M_2$, it must act on $\vec{u} \otimes \vec{v}$, viewed as an element in Euclidean space, as $H(M_1 \otimes M_2)(\vec{u} \otimes \vec{v}) = H(M_1)(\vec{u}) \otimes H(M_2)(\vec{v})$.

With this in mind, when taking any element of from the top left corner of the first square and taking the upper route to the bottom right corner, we see that:

$$(\vec{u}, \vec{v}) \mapsto \vec{u} \otimes \vec{v} \mapsto \vec{u} \otimes \vec{w} \tag{23}$$

Along the bottom route, we have

$$(\vec{u}, \vec{v}) \mapsto (\vec{u}, \vec{w}) \mapsto \vec{u} \otimes \vec{w} \tag{24}$$

Thus the square commutes.

- Hence have shown that there exist two coherence maps ε and μ satisfying the appropriate conditions to make F lax monoidal.

□

For any two doubled ZX diagrams $D_1, D_2 \in ZX_{\ddagger}$, we have $\llbracket D_1 \otimes D_2 \rrbracket = \llbracket D_1 \rrbracket \otimes \llbracket D_2 \rrbracket$. This leads to the following corollary:

Corollary 1. *The functor $\llbracket - \rrbracket_{\ddagger} F$ is lax monoidal.*

This allows us to use doubled ZX diagrams in our hybrid quantum-classical diagrams.

Remark 2. In the context of quantum information, the fact that our functor is lax monoidal but not oplax is not a bug, but a feature. Classical information can be encoded into a quantum system accurately, reflected by the preservation of wires entering the quantum system in our string diagrams. On the other hand, extracting information from the quantum system involves measurement, collapsing the superposition of the quantum state. This yields a probabilistic outcome and is reflected by the bunching up of wires leaving the quantum system into scalar probabilities.

³ G is in fact strict monoidal.

3 Application

In this section we apply our theoretical framework to the quantum machine learning experiments outlined in [14] for the MNIST[22] classification task. In these experiments, a simplified version of the MNIST dataset is used: a subset of two of the 10 digits are chosen, the 28×28 -pixel input images are downsampled to 4×4 and binarized, in the sense that each pixel is then set to either 0 or 1 depending on whether it exceeds a threshold value. This leaves us with images represented by 16-digit binary strings $(x_0, x_1, \dots, x_{15})$, which can be encoded on a quantum computer as states $|x_0x_1 \dots x_{15}\rangle$.

3.1 Quantum Data Encoding

For clarity of exposition, we will draw string diagrams for 4-bit binary strings, from which the case of 16-bit strings follows analogously. Using our hybrid classical-quantum framework, we can explicitly express the encoding of these classical binary string into the quantum system. Take, for example, the string 0100. This would become the quantum state $|0100\rangle$ obtained by applying an X gate to the second qubit, which we can express using the following ZX-diagram:

(25)

In our hybrid string diagrams, quantum systems are contained within functorial boxes[24]. We can thus turn (25) into a hybrid diagram representing the encoding of the classical data 0100 into a quantum state by placing it inside a functor box and ‘pulling out’ the spiders into the classical part of the diagram:

(26)

3.2 Quantum Measurement

The experiment in [14] distinguishes between two different MNIST digit classes by measuring a Pauli operator, such as σ_Z , on single classical readout qubit. We can obtain this particular expectation value from the probability of measuring the state $|0\rangle$ on the readout qubit via $\langle \sigma_Z \rangle = \text{Prob}(|0\rangle) - \text{Prob}(|1\rangle) = 2\text{Prob}(|0\rangle) - 1$. Measuring this probability on, for example, the last qubit of a 3-qubit system can be represented as the following doubled ZX diagram, where we make use of the discard operation provided by the CPM construction:

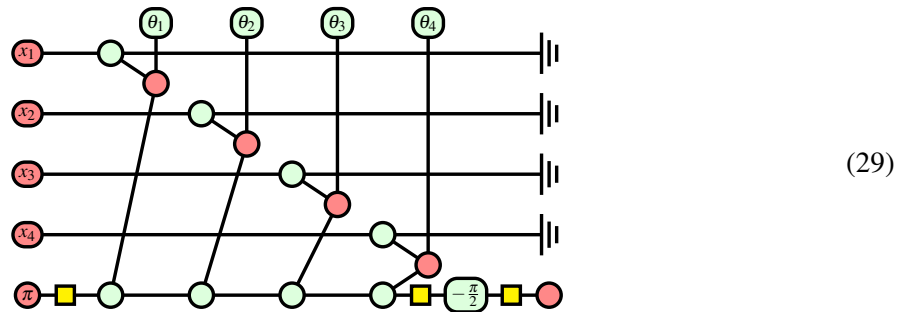
(27)

When contained within a functor box in our hybrid diagrams, this measurement outputs a single wire into our classical system representing a single real number: the measurement probability.

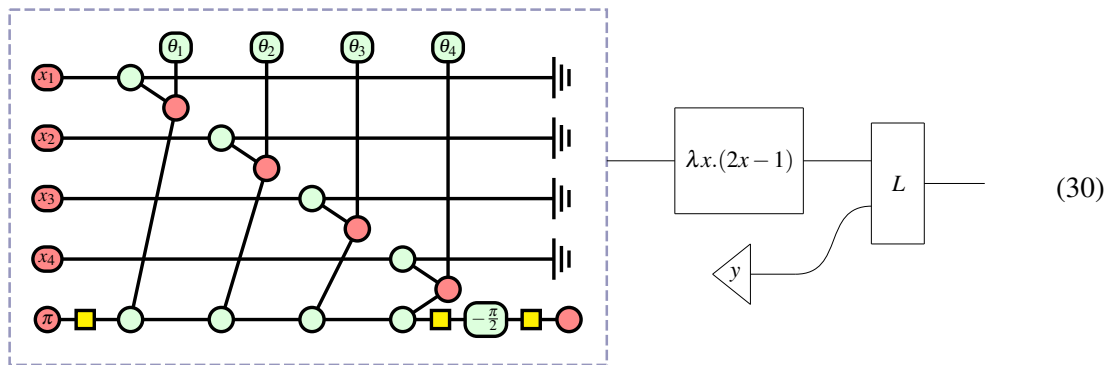


3.3 Quantum Machine Learning with String Diagrams

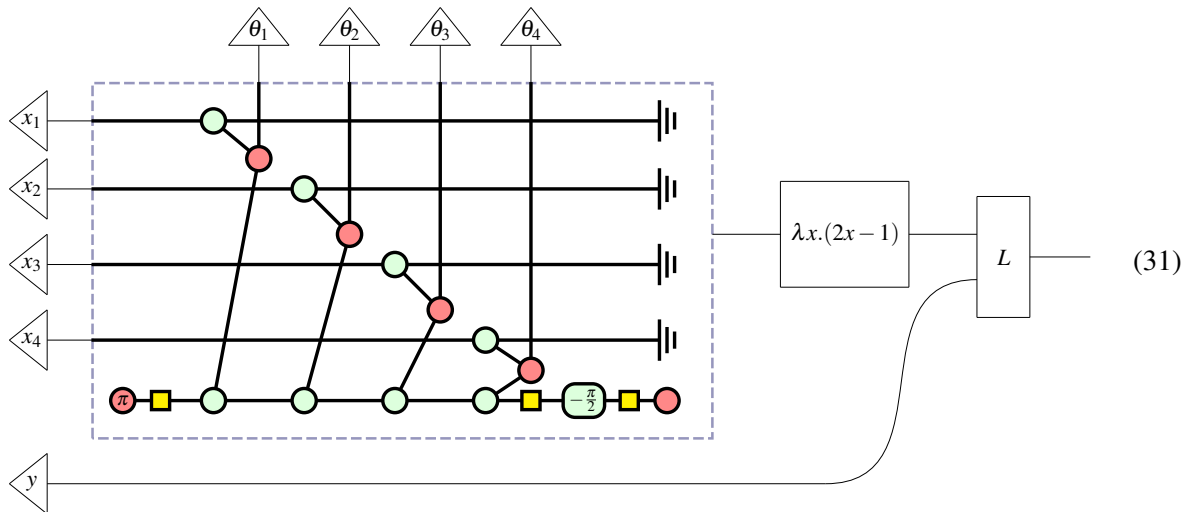
We now present a full hybrid-quantum classical circuit for the experiments in [14] using our framework. The parameterized part of the quantum circuits used consist of ZX and XX interactions, which can be expressed succinctly in the ZX-calculus using ‘phase gadgets’[11]:



Notice that a y-basis measurement is taken on the readout qubit, which was easy to express in ZX diagrams. We can integrate this circuit into our framework by placing it inside a functor box, then composing the output with classical computations for inferring the expectation value and computing a loss function:



Where y represents the label indicating the true class of the input image. We can now pull the relevant spiders out of the box to obtain a diagram that captures the semantics of the hybrid computation by drawing a distinction between classical and quantum parts of the algorithm:



4 Conclusion and Future Work

We have taken initial steps towards a category-theoretic formalism of hybrid quantum-classical machine learning. This was done by embedding the dagger compact closed category $\text{CPM}(\text{FHilb}_{\mathbb{C}})$, in which quantum computation takes place, into a Cartesian category Smooth for the classical computation. This was achieved using a lax monoidal functor, which we defined concretely as the composition of two functors: one from $\text{CPM}(\text{FHilb}_{\mathbb{C}}) \rightarrow \text{Mat}_{\mathbb{R}}$, and another from $\text{Mat}_{\mathbb{R}} \rightarrow \text{Smooth}$. Furthermore, through the use of functor boxes we were able to capture both the classical and quantum part of hybrid algorithms in a single string diagram where functor boxes delineate the quantum-classical interface. A notable consequence of the lax monoidality of our functor was that multiple wires could enter the quantum system when encoding classical data on the quantum computer whereas only one wire, representing a measurement probability, could exit the quantum system. The quantum part of the algorithm could be described as a ZX-diagram, making amenable to quantum circuit optimization methods. Finally, we applied our framework to the MNIST classification task in [14], giving us a denotational semantics of a concrete quantum machine learning algorithm that could form the basis of a programming language.

In future work, we aim to formalise parameterization and backpropagation in these hybrid algorithms using the parametric lens construction of [12]. This will allow for a full specification of a hybrid quantum classical machine learning algorithm with string diagrams capturing both the forward and backward pass. In such a framework, we would need to specify the gradient of quantum parts of the algorithm. This can be done using gradient recipes: quantum circuits that compute the gradients of others. We note the use of the ZXW calculus for computing gradient recipes[21][35] and are interested in employing them in our framework.

5 Acknowledgements

Alexander would like to thank Simon Harrison for the generous support he receives from the Wolfson Harrison UK Research Council Quantum Foundation Scholarship.

References

- [1] *Hybrid computation — PennyLane — pennylane.ai*. https://pennylane.ai/qml/glossary/hybrid_computation/. [Accessed 30-03-2024].
- [2] *The ZX-calculus — zxcalculus.com*. <https://zxcalculus.com/>. [Accessed 12-06-2024].
- [3] Samson Abramsky & Bob Coecke (2004): *A categorical semantics of quantum protocols*. In: *Proceedings of the 19th Annual IEEE Symposium on Logic in Computer Science, 2004.*, IEEE, pp. 415–425.
- [4] Samson Abramsky & Bob Coecke (2008): *Categorical quantum mechanics*. arXiv:0808.1023.
- [5] Reinhold A Bertlmann & Philipp Krammer (2008): *Bloch vectors for qudits*. *Journal of Physics A: Mathematical and Theoretical* 41(23), p. 235303, doi:10.1088/1751-8113/41/23/235303. Available at <http://dx.doi.org/10.1088/1751-8113/41/23/235303>.
- [6] Adam Callison & Nicholas Chancellor (2022): *Hybrid quantum-classical algorithms in the noisy intermediate-scale quantum era and beyond*. *Physical Review A* 106(1), doi:10.1103/physreva.106.010101. Available at <http://dx.doi.org/10.1103/PhysRevA.106.010101>.
- [7] Marco Cerezo, Andrew Arrasmith, Ryan Babbush, Simon C Benjamin, Suguru Endo, Keisuke Fujii, Jarrod R McClean, Kosuke Mitarai, Xiao Yuan, Lukasz Cincio et al. (2021): *Variational quantum algorithms*. *Nature Reviews Physics* 3(9), pp. 625–644.
- [8] JRB Cockett & Robert AG Seely (1999): *Linearly distributive functors*. *Journal of Pure and Applied Algebra* 143(1-3), pp. 155–203.
- [9] Bob Coecke & Ross Duncan (2008): *Interacting Quantum Observables*. In Luca Aceto, Ivan Damgård, Leslie Ann Goldberg, Magnús M. Halldórsson, Anna Ingólfssdóttir & Igor Walukiewicz, editors: *Automata, Languages and Programming*, Springer, Berlin, Heidelberg, pp. 298–310, doi:10.1007/978-3-540-70583-3_25.
- [10] Bob Coecke & Aleks Kissinger (2018): *Picturing quantum processes: A first course on quantum theory and diagrammatic reasoning*. In: *Diagrammatic Representation and Inference: 10th International Conference, Diagrams 2018, Edinburgh, UK, June 18-22, 2018, Proceedings 10*, Springer, pp. 28–31.
- [11] Alexander Cowtan, Silas Dilkes, Ross Duncan, Will Simmons & Seyon Sivarajah (2020): *Phase Gadget Synthesis for Shallow Circuits*. *Electronic Proceedings in Theoretical Computer Science* 318, p. 213–228, doi:10.4204/eptcs.318.13. Available at <http://dx.doi.org/10.4204/EPTCS.318.13>.
- [12] Geoffrey S. H. Cruttwell, Bruno Gavranovic, Neil Ghani, Paul Wilson & Fabio Zanasi (2024): *Deep Learning with Parametric Lenses*. arXiv:2404.00408.
- [13] Samuel Eilenberg & Saunders MacLane (1945): *General theory of natural equivalences*. *Transactions of the American Mathematical Society* 58, pp. 231–294.
- [14] Edward Farhi & Hartmut Neven (2018): *Classification with Quantum Neural Networks on Near Term Processors*. arXiv:1802.06002.
- [15] Brendan Fong, David Spivak & Rémy Tuyéras (2019): *Backprop as functor: A compositional perspective on supervised learning*. In: *2019 34th Annual ACM/IEEE Symposium on Logic in Computer Science (LICS)*, IEEE, pp. 1–13.
- [16] Brendan Fong & David I Spivak (2018): *Seven Sketches in Compositionality: An Invitation to Applied Category Theory*. arXiv:1803.05316.
- [17] Bruno Gavranović: *Category_Theory_Machine_Learning: List of papers studying machine learning through the lens of category theory*. https://github.com/bgavran/Category_Theory_Machine_Learning. [Accessed 11-06-2024].
- [18] Bruno Gavranović, Paul Lessard, Andrew Dudzik, Tamara von Glehn, João G. M. Araújo & Petar Veličković (2024): *Position: Categorical Deep Learning is an Algebraic Theory of All Architectures*. arXiv:2402.15332.
- [19] Lov K. Grover (1996): *A fast quantum mechanical algorithm for database search*. arXiv:quant-ph/9605043.

- [20] Gen Kimura (2003): *The Bloch vector for N-level systems*. *Physics Letters A* 314(5–6), p. 339–349, doi:10.1016/s0375-9601(03)00941-1. Available at [http://dx.doi.org/10.1016/S0375-9601\(03\)00941-1](http://dx.doi.org/10.1016/S0375-9601(03)00941-1).
- [21] Mark Koch (2022): *Quantum Machine Learning using the ZXW-Calculus*. arXiv:2210.11523.
- [22] Yann LeCun, Corinna Cortes & CJ Burges (2010): *MNIST handwritten digit database*. ATT Labs [Online]. Available: <http://yann.lecun.com/exdb/mnist> 2.
- [23] Tom Leinster (2016): *Basic Category Theory*. arXiv:1612.09375.
- [24] Paul-André Melliès (2006): *Functorial boxes in string diagrams*. In: *International Workshop on Computer Science Logic*, Springer, pp. 1–30.
- [25] K. Mitarai, M. Negoro, M. Kitagawa & K. Fujii (2018): *Quantum circuit learning*. *Physical Review A* 98(3), doi:10.1103/physrev.98.032309. Available at <http://dx.doi.org/10.1103/PhysRevA.98.032309>.
- [26] nLab authors (2024): *monoidal functor*. <https://ncatlab.org/nlab/show/monoidal+functor>. Revision 54.
- [27] Alberto Peruzzo, Jarrod McClean, Peter Shadbolt, Man-Hong Yung, Xiao-Qi Zhou, Peter J. Love, Alán Aspuru-Guzik & Jeremy L. O’Brien (2014): *A variational eigenvalue solver on a photonic quantum processor*. *Nature Communications* 5(1), doi:10.1038/ncomms5213. Available at <http://dx.doi.org/10.1038/ncomms5213>.
- [28] Robin Piedeleu & Fabio Zanasi (2023): *An Introduction to String Diagrams for Computer Scientists*. arXiv:2305.08768.
- [29] John Preskill (2018): *Quantum Computing in the NISQ era and beyond*. *Quantum* 2, p. 79, doi:10.22331/q-2018-08-06-79. Available at <http://dx.doi.org/10.22331/q-2018-08-06-79>.
- [30] Maria Schuld, Ville Bergholm, Christian Gogolin, Josh Izaac & Nathan Killoran (2019): *Evaluating analytic gradients on quantum hardware*. *Physical Review A* 99(3), doi:10.1103/physrev.99.032331. Available at <http://dx.doi.org/10.1103/PhysRevA.99.032331>.
- [31] P. Selinger (2010): *A Survey of Graphical Languages for Monoidal Categories*, p. 289–355. Springer Berlin Heidelberg, doi:10.1007/978-3-642-12821-9_4. Available at http://dx.doi.org/10.1007/978-3-642-12821-9_4.
- [32] Peter Selinger (2007): *Dagger compact closed categories and completely positive maps*. *Electronic Notes in Theoretical computer science* 170, pp. 139–163.
- [33] Peter W. Shor (1997): *Polynomial-Time Algorithms for Prime Factorization and Discrete Logarithms on a Quantum Computer*. *SIAM Journal on Computing* 26(5), p. 1484–1509, doi:10.1137/s0097539795293172. Available at <http://dx.doi.org/10.1137/S0097539795293172>.
- [34] P.W. Shor (1994): *Algorithms for quantum computation: discrete logarithms and factoring*. In: *Proceedings 35th Annual Symposium on Foundations of Computer Science*, pp. 124–134, doi:10.1109/SFCS.1994.365700.
- [35] Quanlong Wang, Richie Yeung & Mark Koch (2022): *Differentiating and Integrating ZX Diagrams with Applications to Quantum Machine Learning*. arXiv:2201.13250.
- [36] John van de Wetering (2020): *ZX-calculus for the working quantum computer scientist*. arXiv:2012.13966.

A Appendix

A.1 Categories and Functors

Definition 9 (Category). A category \mathcal{C} consists of the following:

- (i) A collection⁴ of *objects* $\text{Ob}(\mathcal{C})$.
- (ii) For each pair of objects A, B a set $\mathcal{C}(A, B)$ whose elements are called *morphisms* from A to B .
- (iii) For each object A , a morphism $id_A \in \mathcal{C}(A, A)$ called the *identity morphism* for A .
- (iv) For any three objects A, B, C and any two morphisms $f \in \mathcal{C}(A, B)$ and $g \in \mathcal{C}(B, C)$, a morphism $f \circ g \in \mathcal{C}(A, C)$ called the *composite* of f and g .

For notational convenience, we will often objects $C \in \text{Ob}(\mathcal{C})$ as $C \in \mathcal{C}$, and morphisms $f \in \mathcal{C}(A, B)$ as $f : A \rightarrow B$. These constituents are subject to the following conditions:

- (i) For any morphism $f : A \rightarrow B$, composition with the identity gives the same morphism:

$$id_A \circ f = f = f \circ id_B$$

- (ii) For any three morphisms $f : A \rightarrow B$, $g : B \rightarrow C$, $h : C \rightarrow D$ their composition is associative:

$$(f \circ g) \circ h = f \circ (g \circ h)$$

Given this equality, we will write such compositions simply as $f \circ g \circ h$.

Definition 10 (Functor). A *functor* F between two categories \mathcal{C} and \mathcal{D} consists of:

- (i) For each object $C \in \mathcal{C}$, an object $F(C) \in \mathcal{D}$
- (ii) For each morphism $f : A \rightarrow B$ in \mathcal{C} , a morphism $F(f) : F(A) \rightarrow F(B)$ in \mathcal{D} .

Subject to the following conditions:

- (i) Identities are preserved: $F(id_C) = id_{F(C)}$.
- (ii) Composition is preserved: $F(f \circ g) = F(f) \circ F(g)$.

Definition 11 (Natural transformation). Let F and G be functors $\mathcal{C} \rightarrow \mathcal{D}$. A *natural transformation* α is a family of morphisms $\{\alpha_C\}_{C \in \mathcal{C}}$ in \mathcal{D} , such that:

- (i) The family contains exactly one morphism α_C for each object $C \in \mathcal{C}$, which we call *the component of α at C* .
- (ii) For every morphism $f : A \rightarrow B$ in \mathcal{C} , the following diagram in \mathcal{D} commutes:

$$\begin{array}{ccc} F(A) & \xrightarrow{\alpha_A} & G(A) \\ F(f) \downarrow & & \downarrow G(f) \\ F(B) & \xrightarrow{\alpha_B} & G(B) \end{array}$$

Definition 12 (Isomorphism). A morphism $f : A \rightarrow B$ in a category \mathcal{C} is an *isomorphism* if there exists a morphism $f^{-1} : B \rightarrow A$ such that $f \circ f^{-1} = id_B$ and $f^{-1} \circ f = id_A$. The morphism f^{-1} is referred to as the *inverse* of f .

Definition 13 (Natural isomorphism). A natural transformation α is called a *natural isomorphism* if each component α_c is an isomorphism in \mathcal{D} .

Product categories extend the notion of the Cartesian product of sets to categories.

⁴We use collections to avoid Russell's paradox, since objects may themselves be sets.

A.2 Symmetric Monoidal Categories and PROPs

Definition 14 (Product category). Let \mathcal{C} and \mathcal{D} be categories. The *product category* $\mathcal{C} \times \mathcal{D}$ has:

- (i) As objects pairs (C, D) of objects $C \in \mathcal{C}$ and $D \in \mathcal{D}$.
- (ii) as morphisms $(C_1, D_1) \rightarrow (C_2, D_2)$ pairs (f, g) , where $f : C_1 \rightarrow C_2$ is a morphism in \mathcal{C} and $g : D_1 \rightarrow D_2$ is a morphism in \mathcal{D} .

Composition is defined element-wise: $(f_1, g_1) \circ (f_2, g_2) = (f_1 \circ f_2, g_1 \circ g_2)$, and identities are given by pairs of identities from the original categories: $id_{(C, D)} = (id_C, id_D)$.

Product categories allow us to define bifunctors.

Definition 15 (Bifunctor). A *bifunctor* is a functor whose domain is a product category.

Definition 16 (Monoidal Category). A *monoidal structure* on a category \mathcal{C} consists of the following:

- (i) A bifunctor $- \otimes - : \mathcal{C} \times \mathcal{C} \rightarrow \mathcal{C}$ called the *monoidal product*.
- (ii) An object $I \in \mathcal{C}$, called the *monoidal unit*.
- (iii) Three natural isomorphisms:
 - (a) $\alpha : ((- \otimes -) \otimes -) \rightarrow (- \otimes (- \otimes -))$ called the *associator*, with components $\alpha_{A, B, C} : (A \otimes B) \otimes C \rightarrow A \otimes (B \otimes C)$.
 - (b) $\lambda : (I \otimes -) \rightarrow (-)$ called the *left unitor*, with components $\lambda_C : I \otimes C \rightarrow C$.
 - (c) $\rho : (C \otimes I) \rightarrow (-)$ called the *right unitor*, with components $\rho_C : C \otimes I \rightarrow C$.

These constituents are subject to the following *coherence conditions* for all $A, B, C, D \in \mathcal{C}$:

- (i) The *pentagon identity*

$$\begin{array}{ccc}
 & (A \otimes B) \otimes (C \otimes D) & \\
 \alpha_{A \otimes B, C, D} \nearrow & & \searrow \alpha_{A, B, C \otimes D} \\
 ((A \otimes B) \otimes C) \otimes D & & A \otimes (B \otimes (C \otimes D)) \\
 \alpha_{A, B, C} \otimes id_D \searrow & & \swarrow id_A \otimes \alpha_{B, C, D} \\
 (A \otimes (B \otimes C)) \otimes D & \xrightarrow{\alpha_{A, B \otimes C, D}} & A \otimes ((B \otimes C) \otimes D)
 \end{array}$$

- (ii) The *triangle identity*

$$\begin{array}{ccc}
 (A \otimes I) \otimes B & \xrightarrow{\alpha_{A, I, B}} & A \otimes (I \otimes B) \\
 \lambda_A \otimes id_B \searrow & & \swarrow id_A \otimes \rho_B \\
 & A \otimes B &
 \end{array}$$

We call a category with a particular monoidal structure a *monoidal category*. When we want to indicate the particular monoidal structure of a monoidal category, we will write $(\mathcal{C}, \otimes_{\mathcal{C}}, I_{\mathcal{C}})$.

Definition 17 (Symmetric monoidal category). A *symmetric monoidal category* is a monoidal category with an additional natural isomorphism $\sigma : (- \otimes -) \rightarrow (- \otimes -)$, called the *swap map*, with components $\sigma_{A, B} : A \otimes B \rightarrow B \otimes A$ such that:

- (i) For all $A, B \in \mathcal{C}$, $\sigma_{A,B} \circ \sigma_{B,A} = id_{A \otimes B}$. In other words, swapping is self-inverse.
(ii) For all $A, B, C \in \mathcal{C}$, the following diagram commutes:

$$\begin{array}{ccccc} (A \otimes B) \otimes C & \xrightarrow{\alpha_{A,B,C}} & A \otimes (B \otimes C) & \xrightarrow{\sigma_{A,B \otimes C}} & (B \otimes C) \otimes A \\ \downarrow \sigma_{A,B} \otimes id_C & & & & \downarrow \alpha_{B,C,A} \\ (B \otimes A) \otimes C & \xrightarrow{\alpha_{B,A,C}} & B \otimes (A \otimes C) & \xrightarrow{id_B \otimes \sigma_{A,C}} & B \otimes (C \otimes A) \end{array}$$

Definition 18 (Strict monoidal category). When the associator and unitors of a monoidal category are all identity morphisms, the coherence conditions hold automatically. We call a monoidal category for which this is the case a *strict monoidal category*.

Definition 19 (PROP). A *PROP* is a strict symmetric monoidal category with objects the natural numbers and monoidal product on objects given by addition.

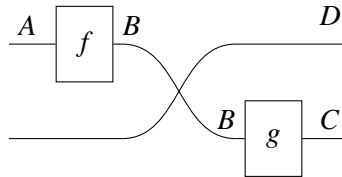
A.3 String Diagrams, Functorial Boxes and Lax Monoidal Functors

A.3.1 String Diagrams

String diagrams are an intuitive, yet formal graphical language with which to express taking arbitrary compositions and tensor products of morphisms in strict monoidal categories. In these diagrams, morphisms are drawn as boxes whose inputs and outputs are connected by wires labelled with objects of the category. The way that the boxes are wired together determines a term created by composing and taking the monoidal product of morphisms in the category. Identity morphisms are drawn as a wire, swap maps are drawn as crossing wires, and the monoidal unit is drawn as an empty diagram. For example, for $f : A \rightarrow B$ and $g : B \rightarrow C$ in a symmetric monoidal category, the term:

$$(f \otimes id_D) \circ \sigma_{B,D} \circ (id_D \otimes g)$$

becomes:



String diagrams represent the same morphism up to topological deformation. This gives rise to a key feature of string diagrams: that they automatically capture the associativity and identity laws for both composition and monoidal product. For composition, associativity becomes:

$$f \circ (g \circ h) = \begin{array}{c} A \quad B \quad C \quad D \\ \boxed{f} \quad \boxed{g} \quad \boxed{h} \\ \hline \end{array} = (f \circ g) \circ h$$

While the identity law $f \circ id_B = f = id_A \circ f$ becomes:

$$\begin{array}{c} A \quad B \\ \boxed{f} \\ \hline \end{array} = \begin{array}{c} A \quad B \\ \hline \boxed{f} \end{array} = \begin{array}{c} A \quad B \\ \hline \boxed{f} \end{array}$$

And similar for the monoidal product, where the diagram composition now occurs in parallel. For further introductions to string diagrams, see [31, 28].

A.3.2 Functorial Boxes

First introduced in [8] and further developed in [24], functorial boxes allow the incorporation of functor application into string diagrams. For a string diagram drawn in some category \mathcal{D} , we can depict a functor $F : \mathcal{C} \rightarrow \mathcal{D}$ applied to a morphism in \mathcal{C} by containing a string diagram for the morphism in \mathcal{C} within a box:

$$\begin{array}{c} F(A) \quad \boxed{F(f)} \quad F(B) \\ \hline \end{array} = \begin{array}{c} \quad \\ \quad A \quad \boxed{f} \quad B \quad \\ \hline \end{array}$$

Note that a wire of type $A \in \mathcal{C}$ becomes a wire of type $F(A) \in \mathcal{D}$ upon exiting the box. These boxes elegantly capture the functor law $F(id_A) = id_{F(A)}$ by allowing us to freely add or remove boxes only containing a wire:

$$\begin{array}{c} F(A) \\ \hline \end{array} \quad \begin{array}{c} F(A) \\ \hline \end{array} = \begin{array}{c} \quad \\ \quad A \quad \\ \hline \end{array}$$

As well as capturing the law $F(f \circ g) = F(f) \circ F(g)$ by allowing us to fuse adjacent boxes:

$$\begin{array}{c} F(A) \quad A \quad \boxed{f} \quad B \quad \boxed{g} \quad C \quad F(C) \\ \hline \end{array} = \begin{array}{c} F(A) \quad A \quad \boxed{f} \quad B \quad F(B) \quad B \quad \boxed{g} \quad C \quad F(C) \\ \hline \end{array}$$

A.3.3 Lax Monoidal Functors

There are subtleties when applying functors to monoidal categories in the way that a functor interacts with the monoidal product. This becomes important for our functorial boxes. For example, $F(A \otimes B)$ may not necessarily equal $F(A) \otimes F(B)$. This gives rise to the notion of lax, oplax and strong monoidal functors. In terms of string diagrams and functorial boxes, this governs the ability to allow whether multiple wires can enter a box, and whether multiple wires exiting a box are preserved as multiple wires or combined into a single wire. In our work, we are interested in lax monoidal functors[26]:

Definition 20 (Lax Monoidal Functor). Let $(\mathcal{C}, \otimes_{\mathcal{C}}, I_{\mathcal{C}})$ and $(\mathcal{D}, \otimes_{\mathcal{D}}, I_{\mathcal{D}})$ be monoidal categories. A *lax monoidal functor* between them consists of:

- (i) A functor $F : \mathcal{C} \rightarrow \mathcal{D}$.
- (ii) *Coherence maps*:
 - (a) A morphism $\varepsilon : I_{\mathcal{D}} \rightarrow F(I_{\mathcal{C}})$ in \mathcal{D} .
 - (b) A natural transformation $\mu : F(-) \otimes_{\mathcal{D}} F(-) \rightarrow F(- \otimes_{\mathcal{C}} -)$, with components $\mu_{A,B} : F(A) \otimes_{\mathcal{D}} F(B) \rightarrow F(A \otimes_{\mathcal{C}} B)$.

These coherence maps are subject to the following conditions:

(i) *Associativity*: for all $A, B, C \in \mathcal{C}$, the following diagram commutes:

$$\begin{array}{ccc}
 (F(A) \otimes_{\mathcal{D}} F(B)) \otimes_{\mathcal{D}} F(C) & \xrightarrow{\alpha_{F(A), F(B), F(C)}^{\mathcal{D}}} & F(A) \otimes_{\mathcal{D}} (F(B) \otimes_{\mathcal{D}} F(C)) \\
 \downarrow \mu_{A, B} \otimes_{\mathcal{D}} id_{F(C)} & & \downarrow id_{F(A)} \otimes_{\mathcal{D}} \mu_{B, C} \\
 F(A \otimes_{\mathcal{C}} B) \otimes_{\mathcal{D}} F(C) & & F(A) \otimes_{\mathcal{D}} F(B \otimes_{\mathcal{C}} C) \\
 \downarrow \mu_{A \otimes_{\mathcal{C}} B, C} & & \downarrow \mu_{A, B \otimes_{\mathcal{C}} C} \\
 F((A \otimes_{\mathcal{C}} B) \otimes_{\mathcal{C}} C) & \xrightarrow{F(\alpha_{A, B, C}^{\mathcal{C}})} & F(A \otimes_{\mathcal{C}} (B \otimes_{\mathcal{C}} C))
 \end{array}$$

Where $\alpha^{\mathcal{C}}$ and $\alpha^{\mathcal{D}}$ denote the associators in \mathcal{C} and \mathcal{D} , respectively.

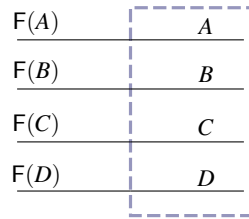
(ii) *Unitality*: for all $C \in \mathcal{C}$, the following diagrams commute:

$$\begin{array}{ccc}
 I_{\mathcal{D}} \otimes_{\mathcal{D}} F(C) & \xrightarrow{\varepsilon \otimes_{\mathcal{D}} F(id_C)} & F(I_{\mathcal{C}}) \otimes_{\mathcal{D}} F(C) \\
 \downarrow \lambda_{F(C)}^{\mathcal{D}} & & \downarrow \mu_{I_{\mathcal{C}}, C} \\
 F(C) & \xleftarrow{F(\lambda_C^{\mathcal{C}})} & F(I_{\mathcal{C}} \otimes_{\mathcal{C}} C)
 \end{array}$$

$$\begin{array}{ccc}
 F(C) \otimes_{\mathcal{D}} I_{\mathcal{D}} & \xrightarrow{F(id_C) \otimes_{\mathcal{D}} \varepsilon} & F(C) \otimes_{\mathcal{D}} F(I_{\mathcal{C}}) \\
 \downarrow \rho_{F(C)}^{\mathcal{D}} & & \downarrow \mu_{C, I_{\mathcal{C}}} \\
 F(C) & \xleftarrow{F(\rho_C^{\mathcal{C}})} & F(C \otimes_{\mathcal{C}} I_{\mathcal{C}})
 \end{array}$$

Where $\lambda^{\mathcal{C}}$, $\rho^{\mathcal{C}}$ and $\lambda^{\mathcal{D}}$, $\rho^{\mathcal{D}}$ are the unitors in \mathcal{C} and \mathcal{D} , respectively.

The significance of being lax monoidal in the context of functorial boxes is that it allows for multiple wires to enter a box, which are preserved as multiple wires. This is illustrated by the following:

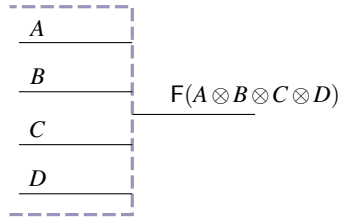


Without the lax monoidal condition, only one wire could enter each box. As there would not be a sensible notion of multiple wires entering, any diagram containing such would be considered ill-formed.

An oplax monoidal functor is defined similarly to a lax monoidal functor, except the coherence maps go in the other direction:

$$\eta : F(I_{\mathcal{C}}) \rightarrow I_{\mathcal{D}} \qquad \nu : F(- \otimes_{\mathcal{C}} -) \rightarrow F(-)$$

An oplax monoidal functor allows multiple wires exiting a box to be preserved as multiple wires. If this is not the case wires exiting are bundled together into a single wire as follows:



If the coherence maps are all isomorphisms for either a lax or an oplax monoidal functor, it is called a strong monoidal functor, and multiple wires can both enter and exit the functorial boxes.